High-Aspect-Ratio Photoresist Processing for Fabrication of High Resolution and Thick Micro-Windings

Ricky Anthony[1, 2*], Elias Laforge[1], Declan P. Casey[1], James F. Rohan[1] and Cian O'Mathuna[1, 2]

[1]Micro-Nano Systems Centre, Tyndall National Institute, University College Cork, Lee Maltings, Cork, Ireland
[2]Electrical and Electronics Engineering, University College Cork, Cork, Ireland

[*]E-mail: ricky.anthony@tyndall.ie

Abstract

DC winding losses remain a major roadblock in realizing high efficiency micro-magnetic components (inductors/transformers). This paper reports an optimized photoresist process using negative tone and acrylic based THB-151N (from JSR Micro), to achieve one of the highest aspect ratio (17:1) and resolution (~ 5 µm) resist patterns for fabrication of thick (~ 80 µm) micro-winding using UV lithography. The process was optimized to achieve photoresist widths from 5 µm to 20 µm with resist thickness of ~ 85 µm in a single spin step. Unlike SU-8, this resist can be readily removed and shows a near-vertical (~ 91^0) side-wall profile. Moreover, the high resolution compared to available resist processes enables a further reduction in the footprint area and can potentially increase the number of winding thereby increasing the inductance density for micro-magnetic components. Resistance measurements of electroplated copper winding of air-core micro-inductors within the standard 0402 size (0.45 mm^2 footprint area) suggested a 42 % decrease in resistance (273 mΩ to 159 mΩ) with the increase in electroplated Cu thickness (50 µm to 80 µm). Reduction of the spacings (10 µm to 5 µm) enabled further miniaturisation of the device (0.60 mm^2 to 0.45 mm^2) without significant increase in resistance.

Keywords: Photolithography, High aspect ratio, High resolution, Micro-windings, MEMS, Integrated Magnetics.

I. Introduction

In recent years, miniaturization of micro-electromechanical systems (MEMS) and advances in chip level packaging has been supported by developments in technologies such as photoresists for patterning via electroplating and wet-etching. MEMS inductors in particular have shrunk from bulky modules into co-packaged micro-scale devices [1]. In the near future, it is predicted that these devices will be completely integrated with power management ICs (PMICs). However, reducing the size below the industry scale 0402 package size (1005 metric, 0.5 mm^2) will only be possible by reducing the feature sizes and increasing packaging density. Metal moulding processes for fabricating inductor micro-windings are presently limited by low resolution photoresist processes. Moreover, miniaturization has shown an increase in DC winding loss contribution [2]. This restricts the net efficiency of the DC-DC converter circuitry. However, it is possible to reduce DC winding losses by increasing winding cross-section area while increasing the filling factor by reducing inter-winding gaps. Furthermore, the need for efficient alternatives to existing MEMS processes especially for selective wet-etching thick metal patterns, moulds in micromachining processes and bump-bonding requires new thick photoresist process development. One of the challenges is to develop a high resolution and high-aspect-ratio (HAR) removable metal moulding photoresist process. For an industrial scale development, the process must be repeatable with an acceptable process margin and stability.

X-Ray-*LIGA* (*Lithographie, Galvanoformung, Abformung*) has been used to achieve high resolution and structure density [3]. However, UV-*LIGA* methods are more attractive being more cost-effective and capable of processing at the dimensions ideal for a wide range of MEMS applications. Negative tone and epoxy type resists such as UV-sensitive SU-8 is one such widely used photoresist in MEMS fabrication processing. The main constituents of SU-8 are octa-functional polymeric epoxy resin, gamma-butyrolactone solvent and tri-arylsulfonium hexa-fluoroantimonate salt as photo-initiator [4]. It utilises solvent based developers such as Propylene Glycol Monomethyl Ether Acetate (PGMEA). Ultrahigh thickness > 1 mm [5] and HAR (> 18) in a single spin [6] have already been reported with SU-8. However, internal stress, low resolution and in some cases poor substrate adhesion [7] are major drawbacks. Moreover, SU-8 swelling during the development step can result in device failure followed by complete delamination [8]. This is often compensated for with adhesion promoters (such as omnicoat) or additives to SU-8. Moreover, processing to improve the adhesion can lead to difficulties in stripping the resist after polymerization which can damage micro-structures. Other chemically amplified ultra-thick photoresists such as KMPR-100, have shown similar drawbacks [9]. Positive tone photoresists such as the AZ series can be readily stripped. However, limited thickness (< 50 μm) [10] and the need for multi-step spin coating steps for higher thickness requirements increases the process time. Furthermore, process optimization becomes difficult as multiple soft bakes have to be included, which means the first coated photoresist layers may be overbaked. An ideal alternative would be a thick negative tone photoresist with appropriate chemistry that permits easy stripping.

As a solution to these drawbacks, we investigated a process for the fabrication of HAR (17:1) micro-windings for MEMS inductor applications. THB-151N (JSR Micro) is a negative tone acrylic based photoresist. Unlike chemically amplified resists (CAR) it requires no post-exposure bake and polymerizes rapidly on UV exposure. Moreover, the resist has excellent adhesion to most metal surfaces, is easy to strip after exposure and has a short soft-bake and exposure dose. An optimized 85 µm thick photoresist process with 5 µm feature width was developed. A critical dimension calculation indicates that 5 µm is the best feature size attainable with 85 µm resist thickness in broad-line UV (g-h-i line) exposure in hard contact mode. Resistance of the electroplated copper windings measured at 75 kHz suggested a sharp decrease with the increase in winding thickness from 50 µm to 80 µm. To our knowledge, this is the highest aspect ratio to be reported with THB-151N and one of highest with small feature sizes using commercially available temporary resists.

II. Experimental Details

The study aimed to develop HAR photoresist patterns for the electrodeposition of inductor micro-coils and identify any limitations associated with the resist. In this work, 575 µm thick 100 mm diameter silicon (100) substrates were used and on which a 1 -2 µm silicon oxide layer was thermally grown to isolate the windings from the substrate. The wafers were sputtered with 99.99% pure Ti adhesion layer (20 nm) and conductive Cu seed layer (200 nm) in a hybrid DC Magnetron tool (Nordiko Ltd.) in an Ar atmosphere. The resist and electroplated Cu patterns were analysed with an FEI Quanta FEG 600 scanning electron microscope system (SEM).

(a) Lithography Process

THB-151N (from JSR Micro Inc.) is a semi-transparent (clear yellow) viscous (3900 cP at 25^0C) solution mainly constituting 30-40 % propylene glycol monoethyl ether acetate (PGMEA), 30-40% hydroxystyrene (meth)-acrylate copolymer and photosensitizer (~ 8%). The datasheet obtained from manufacturer suggests 7.25 as the highest aspect ratio that could be obtained. The resist is sensitive to broadband UV wavelengths, with peak sensitivity to i-line wavelength (365 nm) and compatible with typical Cu electroplating solutions. It can also be re-flowed to achieve dome like topography by standard baking after development. Prior to spin coating, the resist is allowed to warm to room temperature and exposed to the air briefly to assist natural out-gassing from the photosensitizer often trapped in the solvent.

The AR mentioned for walls by JSR datasheet is 7.25 on 150 mm diameter Cu coated wafers. On repeating the process recommended by JSR for 80 µm resist thickness (spin coating: 300 rpm/10 sec to 950 rpm/20 secs) on 100 mm Cu coated wafers we could achieve an aspect ratio ~ 6.5 and resist thickness 65 µm. Also, following the same bake times we found the solvent content to be too high which made the wafer stick to the chrome mask on hard exposure. This necessitated process optimization for

the 100 mm diameter wafers in terms of spin profile, exposure and bake conditions. The resist was manually dispensed at the centre of the wafer and held for 120 s prior to spin coating on a Laurel spinner (Model-WS-400P-6NPP/LITE/AS). The optimized resist thickness in terms of main spin speed is show in fig. 1 (a). To achieve thickness > 75 µm we reduced the main spin speed to 650 rpm/30 seconds and included sufficient relaxation time before main spin step. The brief relaxation time between pre-spin and main spin allows the resist to re-flow towards the centre from the wafer edges. Decreasing spin speeds further did not yield any increase in thickness but instead exhibited non-uniformity across the wafer. Fig.1 (b) shows the optimized spin profile for different thicknesses. However, high solvent content with lower spin speeds could reduce resist resolution, may result in resist loss during development and can also result in the wafer sticking to the chrome mask during exposure. Hence, the pre-exposure bake time was also optimized. We included 600 secs relaxation time before pre-exposure bake. It was then soft-baked (pre-bake) on a standard hotplate by ramping up to 130 ^{0}C for 600 s (for 85 µm resist thickness) before ramping back down to room temperature. Unlike the process described in the datasheet, the ramped prebake mode ensured no bubbles are formed. However, low temperature bake (< 80 ^{0} C) showed resist loss during development step. The wafer was then exposed (exposure dose: 1100 mJ/cm^{2}) in a high intensity (32 mW/cm^{2}) UV broadband (i-g and h-line mercury lamp) optical mask aligner (Karl Suss MA6 system) through a chrome patterned glass mask (from Compugraphics Ltd., UK) in hard contact mode. We believe shorter exposure dose reduces diffraction from mask edges which effects the resist resolution. No post-baking was needed for THB-151N. The exposed wafer was then developed in puddle mode in the commercial TMA238WA solution (from JSR Micro) at room temperature. It is a metal-ion free (MIF) transparent solution with 2.38% strength by weight alkali tetramethylammonium hydroxide (TMAOH). The thickness across the wafer was measured using an Alphastep-500 surface profilometer. The wafer was nitrogen dried completely. The thick resist structures showed no deformity of collapse on drying, indicating excellent adhesion between the photoresist and Cu surface. It was noticed that the resist wall collapses on under-exposure (700 mJ/cm^{2} as given in datasheet) (fig. 1 (c)) during the development stage. While, longer soft-bake durations (130 ^{o}C > 20 minutes) increased the development time and reduced resolution (fig. 1 (e)).

Table-1 lists the optimized process conditions for 100 mm wafers. Noticeable advantages are the short soft-bake time and the low exposure doses for quick polymer hardening and high UV sensitivity. Also, the development time is dependent on the thickness of the photoresist. This is attributed to the fact that for thicker profiles the developer solution is unable to wet finer or recessed patterns. It also indicates the large process margin with THB-151N.

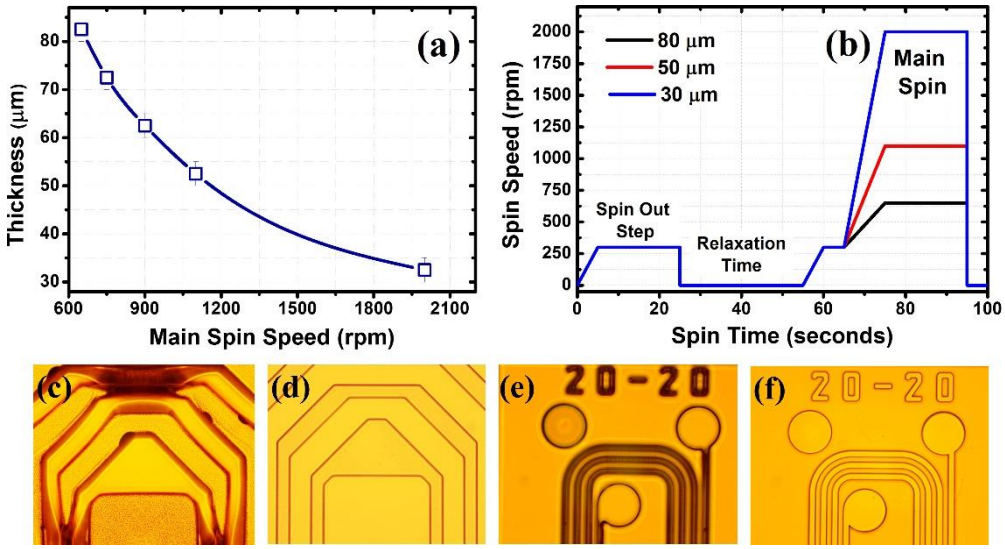

Fig.1. Experimentally determined optimized (a) spin speeds (main) and (b) spin profile for different thickness of THB-151N. Exposure dose and soft-bake optimization (80 μm process): (a) Under-exposed (< 700 mJ/cm^2) (b) optimized exposure (1100 mJ/cm^2) (c) over baked (130 ^{o}C for 30 mins) (d) optimized soft-bake (ramped to and from 130 ^{o}C /10 mins).

Table 1. Optimized process conditions for processing THB-151N photoresist on 100 mm wafer substrates.

Photoresist Thickness (μm)	Spin Speed (rpm) / spin time (sec)	Soft-bake temperature (^{o}C) / duration (min)	Exposure dose (mJ/cm^2)	Development Time (mins)
32.5 ± 2.5	2000 / 30	120 / 5	550	4
52.5 ± 2.5	1100 / 30	130 / 5	700	5
82.5 ± 2.5	650 / 30	Ramped to 130 / 10	1100	9-15

(b) Copper Electroplating and Photoresist strip

The wafer was briefly dipped in an acid-based solution to remove cuprous oxide and improve wettability prior to electroplating Cu. That was followed by a brief O_2 plasma treatment for 2 minutes at 100 W to remove any organic residue. The wafer was then electroplated in an automated wafer plating system (Digital Matrix (SA/1b) system) in 0 pH commercial Cu plating bath (Schlötter Ltd) at room temperature. The deposit thickness was controlled and maintained at each stage to avoid over-plating. After electroplating, the photoresist was removed with THB-S17 (from JSR Micro) metal-ion free solution which constitutes of 89-95% Dimethylsulphoxide at room temperature. The solution was agitated gently during resist removal. The Ti/Cu seed layers were then etched in hydrofluoric acid (HF) and ammonium persulphate solutions, respectively.

III. Results and Discussion

(a) Resist Characterization

It is important to note that in shadow exposure mode the UV exposure plays a crucial role in determining the minimum resolution (the critical dimension (CD)) that can be developed. It is dependent on UV wavelength (λ), the gap between the mask and photoresist (g_{air}) and photoresist thickness (t) and given by [11]:

$$Critical\ Dimension = \frac{3}{2}\sqrt{\lambda\left(g_{air} + \frac{t}{2}\right)} \quad (1)$$

Fig. 2(a) is a schematic depiction of edge broadening observed on UV exposure in hard-contact mode ($g_{air}=0$). The photoresist is more responsive to i-line and hence the optimum λ is considered to be 365 nm. In the case of a negative tone photoresist, the broadening of exposed regions would mean an increase in exposed resist width by 2δ. This means that the minimum width of the dark region (w) should be $>2\,\delta$ to avoid bulk exposure. After exposure, the negative tone resist will broaden to $2\delta+d_{light}$ where 'd_{light}' is the width of the feature size. The situation can worsen in the presence of edge beads which creates an unavoidable mask to resist gap even in hard-contact mode.

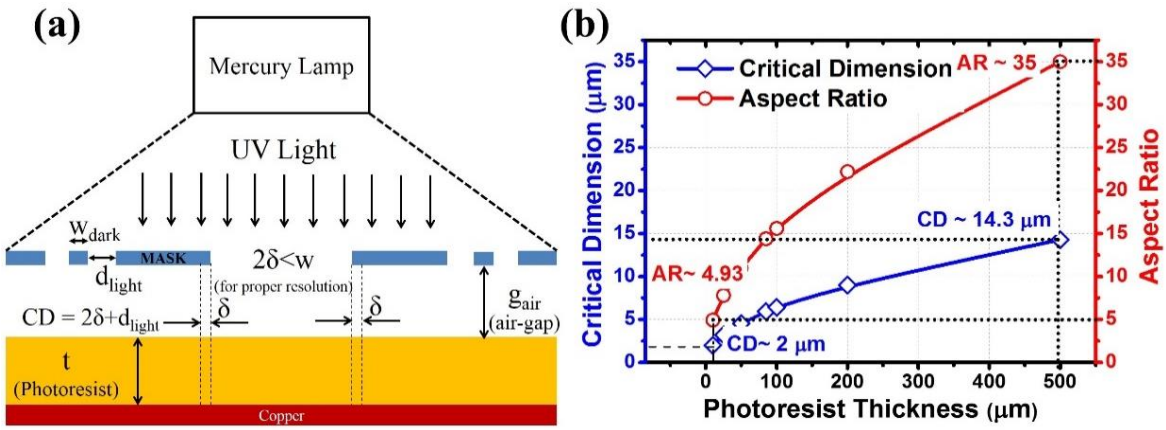

Fig.2. (a) Schematic diagram of thick photoresist exposed by UV light through a photo mask. (b) Critical dimension and maximum aspect ratio with respect to photoresist thickness.

Fig. 2(b) shows minimum resolution and maximum AR achievable in hard-contact mode on UV exposure with photoresist thickness. The AR is calculated by the ratio of photoresist thickness and width by considering the CD as the minimum resist width (for negative tone photoresist). As expected the CD increases with the thickness of the photoresist, but it is interesting to note that the maximum achievable AR also increases with photoresist thickness. For ultra-thick resists (such as SU-8), an AR of 35:1 is possible with 500 µm thickness. This reduces to 2:1 when thickness approaches ~10 µm. It is apparent that thick resist processes are preferable for HAR. However, an increase in thickness also increases the critical dimension significantly as observed from the figure. It is therefore obvious, that a trade-off

exists and must be addressed to ensure a specified footprint area is maintained by opting for an appropriate thickness.

Fig. 3(a) shows the uniformity measured across a 100 mm (4 inch) wafer with THB-151N. Edge beads were avoided by removing the edge resist prior to soft-bake and exposure. This improved the resist uniformity achieving a 3.5 % variation across the wafer. Fig 3(b) shows an 85 µm thick single spin resist coated wafer with different windings patterns. Introducing a short delay between each step and optimizing the soft-bake temperature ensures that bubbles due to de-gassing do not occur.

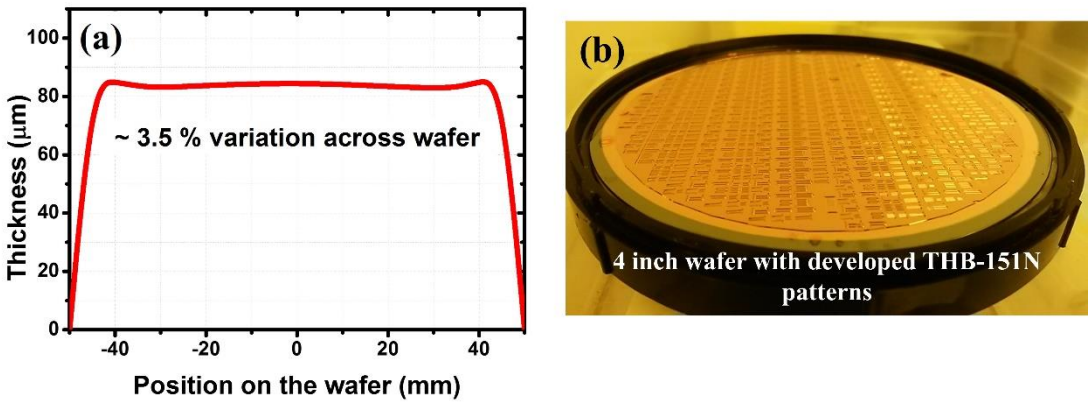

Fig.3. (a) Photoresist thickness measured across a 100 mm diameter wafer and (b) Thick (85 µm) resist with different winding patterns.

The mask design has winding widths varying from 15 µm to 50 µm with windings gaps (or resist width) ranging from 5 µm to 25µm. Fig.4 shows the SEM images of cleanly developed patterns with varying widths and spacing. It was observed that high exposure doses for a short durations improved the resolution significantly. This is attributed to Fresnel diffraction from the mask pattern which degrades resolution during extended exposure. On increasing the exposure time these edges absorb enough light to remain undeveloped. The resist was exposed in hard contact mode. It is also important to note that some features develop earlier than others. This is attributed to the fact that it is difficult to dissolve and remove finer spaced features with the developer solution. However, the relatively large development margin allowed all the patterns to be developed cleanly. Even though the resist shows some swelling before removal during the development, unlike some resists (such as SU-8) [12], it did not deform nearby microstructures.

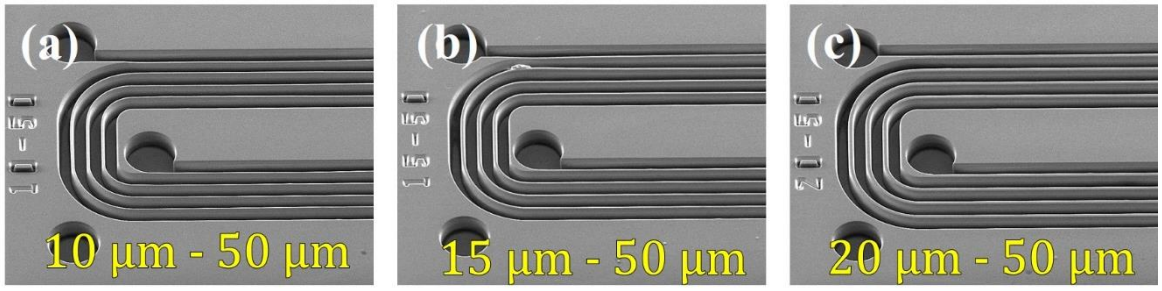

Fig.4. SEM micrographs of 85 µm thick and 50 µm wide open photoresist patterns: (a) 10 µm resist wall width (b) 15 µm resist width and (c) 20 µm resist width.

Fig 5 shows SEM images of 85 µm thick THB-151N resist. Fig. 5(a) shows the 5 µm resist line-width winding patterns with 50 µm resist spacing. As observed the resist is cleanly developed confirming optimized development conditions. No delamination or peeling is observed which confirms excellent adhesion between Cu seed and the resist. Moreover, the tilted image shows a near vertical side-wall profile which is later confirmed with cross-section analysis of electroplated windings. It is important to note that, under-exposure can cause resist loss during the development step while over-exposure results in a negatively sloped side-wall profiles. We have also been able to realize a 17:1 AR with a resist width of 5 µm which is higher than the estimated AR of 14.5 for 85 µm thick resist. Moreover, the resist width of 5 µm is comparable to 5.91 µm resolution determined by CD calculations of the same resist thickness (85 µm). We believe that apart from wavelength and numerical aperture of the exposure tool, the intensity and duration of exposure also plays a crucial role in determining the diffraction intensity from mask edges. A high intensity for short exposure duration, would increase the resolution compared to low intensity for high exposure duration. This permits a clean photoresist development to achieve high resolution patterns. We have observed poorer resolutions (≥ 10 µm resist width) on high exposure duration with low intensity compared to high intensity and short exposure duration (≥ 5 µm). Fig. 5(c) shows the SEM micrograph of 85 µm thick and 10 µm wide resist patterns confirming the near vertical side-wall profile (~ 90^{o}).

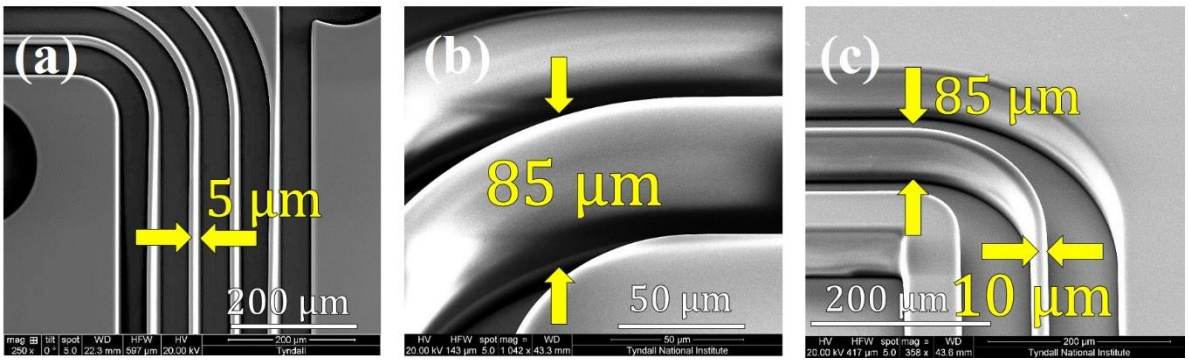

Fig 5. SEM micrographs of ~85 µm thick and 50 µm wide photoresist patterns: (a) 5 µm resist width (b) 85 µm thick resist side-wall and (c) 10 µm resist width resist pattern.

Fig. 6 depicts the SEM images of 80 µm thick electroplated Cu windings with 16:1 aspect ratio via resist mould. It is often experienced that electroplating via inclined resist mould could result in over-plating. As observed from fig. 6 (a-b), the windings are uniformly plated. This can be attributed to uniform width of the resist and near vertical size-walls. Moreover, 5 µm spacing in-between Cu windings demonstrates clean stripping of the resist in 20 mins. None of the Cu microstructures were damaged during the process. This is confirmed with ~80 µm thick vertical features and ~ 5 µm gap (as shown in fig 6(c-d)). Similarly, fig. 7 (a-c) shows the electroplated Cu windings with 10 µm width and 80 µm thickness and again the resist in-between windings is cleanly stripped. The side-wall of electroplated Cu structures is almost 91^{o}.

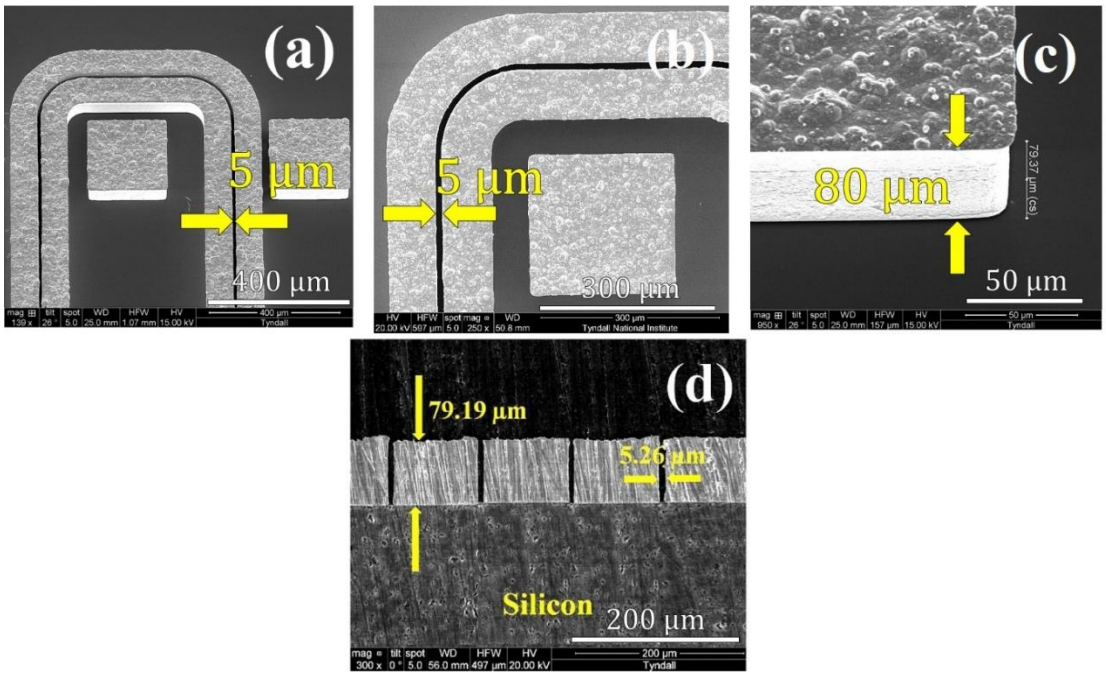

Fig.6. SEM micrographs of electroplated Cu windings depicting: (a-b) 5 µm winding gap and (c-d) 80 µm thick Cu pads and ~91^{0} side-wall profile and 5 µm winding gaps.

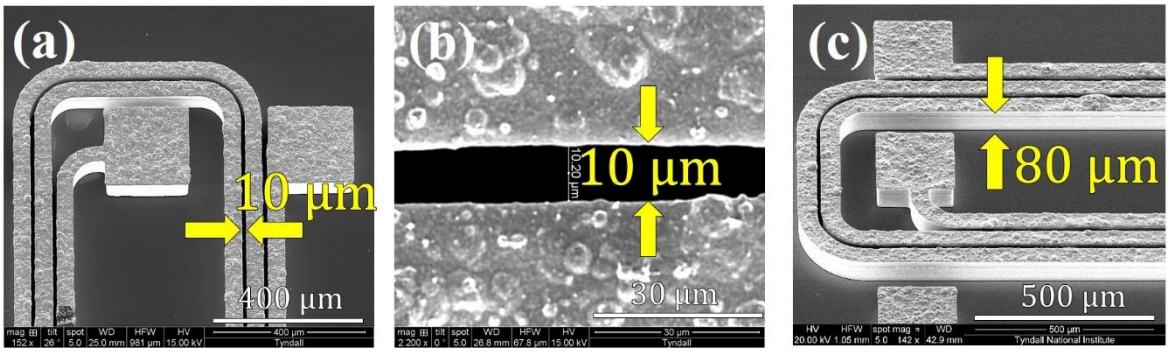

Fig.7. SEM micrographs of electroplated Cu windings: (a-b) 10 µm winding gap and (c) 80 µm thick electroplated Cu windings.

Table 2 lists the thick photoresist processes used for metal moulding applications and compares the process parameters from the literature with the process for THB-151N. As observed from the table, compared to other processes, this process has the shortest time. Positive tone resists need multiple spins

[4] to attain > 50 µm thus increasing the process time to 420 minutes. Moreover, most negative tone resist require significant pre and post exposure bake. Some earlier works have shown encouraging resist thicknesses in single spin processing, however poor resolution [13-14] deems them impractical for miniaturized MEMS fabrication. Furthermore, low ARs are unsuitable for thick MEMS structures [13, 15-16]. Compared to the reported optimized process this work provides HAR and the highest resolution. Advantages of the process developed include lower UV exposure energies, shorter baking times, and excellent adhesion to metal surfaces, vertical side-wall profiles and easy resist removal which make THB-151N ideal for micro-coil processing MEMS applications described here.

Table 2. Comparison of high aspect ratio non-permanent photoresists.

Photoresist	Photoresist Type	Maximum Thickness (µm)/ Number of spin	Minimum Resolution (µm)	Net Pre &Post Bake Time (min)	Aspect ratio
AZ 9260 [10]	Positive tone	81 /4	14	150 / NA	6
BPR 100[13]	Negative tone	100 /1	60	40 / 20	1.5
BPN 100[14]	Negative tone	500 /-	30	425 / NA	17
NR2-20000P [15-16]	Negative tone	120/-	-	-	3
THB-151N [17-18]	Negative tone	58/1	10	15 / NA	5.8
AZ 125XT [19]	Negative tone	400 /-	30	855 / -	< 14
THB-151N [This work]	Negative tone	85/1	5	25 /NA	17

(b) Winding Specifications

One prominent area of application for AR moulding resist patterns is the fabrication of micro-windings for RF MEMS components (such as micro-inductors and micro-transformers) which are increasingly being integrated in power converters, filters, oscillator circuits etc. Fig. 8 (a) depicts the schematic of magnetic core micro-inductor cross-section. The performance indicative parameter of these devices is the *Q*-factor which is dependent on the resistance (*R*) and inductance (*L*) of the windings at frequency (*f*) and given by:

$$Q = {}^{2\pi fL}/_{R} \tag{2}$$

In order to achieve high performance characteristics, it is apparent that the resistance has to be reduced for a designed inductance within a designated footprint area. This is only feasible with a high AR and high resolution moulding photoresist process respectively. Thick micro-windings decrease DC resistance which increases the Q-value [20]. Fig 8(b) depicts an analytical study of micro-inductor efficiency with varying windings spacing and width for 50 µm and 80 µm thick Cu windings (4 turn) with magnetic core. The footprint area (0.5 mm^2), device geometry, frequency (20 MHz) and core losses have been fixed to explicitly study the influence of eddy current losses due to variation in winding geometry on device efficiency. Increasing winding width at the expense of winding spacing improves device efficiency while the efficiency of the device can be further improved by increasing winding thickness. However, the resolution of the photoresist process often restricts the windings spacing. While high AR processes have been reported previously, very few attempts have been made to achieve high resolution along with such thicknesses.

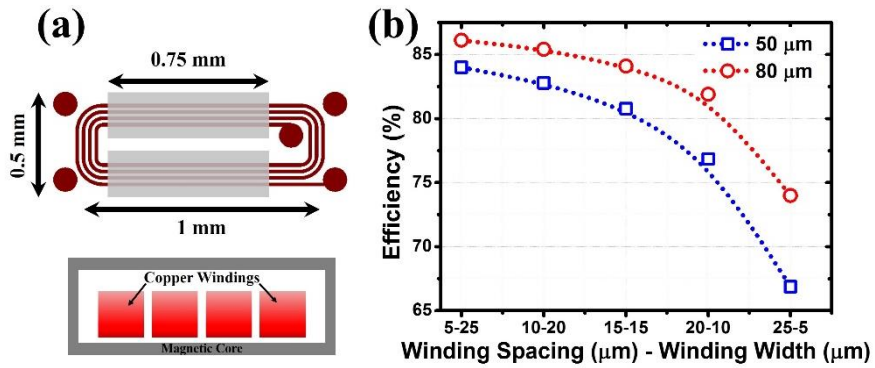

Fig.8. (a) Schematic representation of a magnetic core micro-inductor and its cross-section. (b) Influence of winding thickness and width on micro-inductor efficiency (0.5 mm2 footprint area).

Table-3 lists the air-core micro-inductors fabricated at wafer-scale with the footprint area and the measured small-signal resistances (75 kHz-30 MHz, HP 4285 LCR meter). On comparing with previous reported processes [16], (inductors with ~ 12 nH designed inductance at 75 kHz) the resistance of 50 µm thick windings and 10 µm spacing (0.45 mm^2 footprint area), with 80 µm height windings and 5 µm spacing (0.39 mm^2 footprint area) suggested ~ 42 % reduction at 75 kHz for 20 µm wide windings (fig.9 (a)). This is attributed to the increase in winding cross-sectional area which varies inversely with resistance. At low frequencies (such as 75 kHz), the effective cross-sectional area determined by skin depth (~ 238 µm) is larger than the winding cross-section. Hence, AC losses are negligible <1 MHz (as observed from fig. 9(a)). However, at high frequencies the winding resistance increases due to reduced effective area (skin effect) and proximity effects. The proximity effect can be reduced by increasing the winding spacing but that would also increase the device footprint area. Nevertheless, as a trade-off the footprint area can be reduced further with the new process by decreasing winding spacing with a small increase in resistance (fig 9 (b)) at high frequency. Another advantage of the high resolution achieved with this process is to increase the number of turns per footprint area, thereby increasing the inductance density. Such compact MEMS devices could easily be integrated on-chip. Moreover, such high AR photoresist processing could also be applicable in the fabrication of MEMS and interconnect applications. To the authors knowledge it is one of the highest AR achieved for moulding photoresist (that is readily removable) with such high resolution.

Table 3. Footprint area and measured resistances of 80 µm thick 4-turn micro-windings at 75 kHz.

Package Size	Footprint Area (mm^2)				Resistance (Ohm)			
	Winding width (µm)	Winding Gap (µm)			Winding width (µm)	Winding Gap (µm)		
		5	**10**	**15**		**5**	**10**	**15**
0402	**15**	0.36	0.39	0.45	**15**	0.20	0.22	0.23

	20	0.39	0.45	0.50	**20**	0.16	0.17	0.18
	25	0.45	0.55	0.60	**25**	0.134	0.15	0.16
		5	**10**	**15**		**5**	**10**	**15**
0603	**15**	0.53	0.58	0.65	**15**	0.237	0.25	0.26
	20	0.58	0.65	0.74	**20**	0.193	0.20	0.21
	25	0.65	0.74	0.82	**25**	0.16	0.17	0.18
		10	**15**	**20**		**10**	**15**	**20**
0805	**50**	1.68	1.78	1.9	**50**	0.14	0.146	0.154

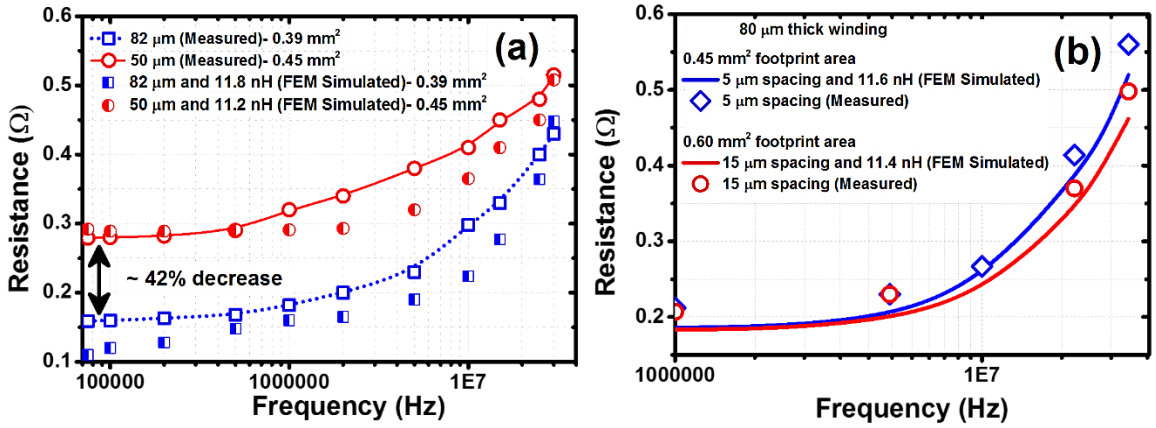

Fig. 9. Winding resistance vs frequency comparisons: (a) Increase in winding thickness (from 50 µm to 82 µm) and reducing footprint area (from 0.45 mm^2 to 0.39 mm^2) by reducing winding spacing. (b) Reduction of device footprint (0.60 mm^2 to 0.45 mm^2) with new high resolution resist process without significant increase in resistance.

IV. Conclusion

This work demonstrates a new high resolution and high aspect ratio photoresist optimized process for fabrication of micro-windings in MEMS applications with negative tone THB-151N. Lithography parameters were optimized to achieve 35 µm to 85 µm photoresist thickness in a single spin. This includes exposure dose, baking condition and development time optimization. Thick copper micro-windings (~80 µm) with varying winding width (5 µm to 25 µm) and footprint area (0.36 mm^2-1.9 mm^2) were fabricated for integrated power magnetic devices (such as micro-inductors and micro-transformers). The resistance of 80 µm thick windings and 5 µm spacing (0.39 mm^2) suggested ~ 42 % reduction (from 273 mΩ to 159 mΩ) measured at 75 kHz compared to 50 µm thick windings and 10 µm spacing (0.45 mm^2). The high resolution process ensures further reduction in winding pitch and device miniaturization without significant concessions on efficiency. The near-vertical side-wall profile assists the control of the copper electroplating rate. Unlike ultra-thick photoresists such as SU-8, this photoresist can be easily stripped after exposure. Higher single spin thickness by comparison with positive tones photoresists reduces processing time while increasing process margin and resolution. This resist process is appropriate for applications in MEMS for micro-fabrication of high AR and low loss micro-windings.

Acknowledgement

The authors would like to acknowledge JSR Micro for providing THB-151N, the European Commission for funding the research through EU PowerSwipe (Grant Agreement No.: 318529) and the Central Fabrication Facilities (CFF) at Tyndall National Institute for assistance.

References

[1] O' Mathúna C, Wang N, Kulkarni S and Roy S 2012 Review of integrated magnetics for power supply on chip IEEE T. Magn. **27** 4799-4816.

[2] Meere R, O' Donnell T, Wang N, Achotte N, Kulkarni S and O' Mathúna S C 2009 Size and performance trade-offs in micro-inductors for high frequency DC-DC conversion **45** 4234-4237.

[3] Kim S H, Lee S H and Kim Y K 2002 A high-aspect-ratio come actuator using UV-LIGA surface micromachining and (110) silicon bulk micromachining **12** 128-135.

[4] Zhang J, Chan-Park M B and Li C M 2008 Network properties and acid degradability of epoxy-based SU-8 resists containing reactive gamma-butyrolactone Sensor Actuat. B-Chem. **131** 609-620.

[5] Lorenz H, Despont M, Fahrni N, Brugger J, Vettiger P and Renaud P 1998 High-aspect-ratio, ultra-thick, negative-tone-near-UV photoresist and its applications for MEMS Sensor Actuat. A-Phys. **64** 33-39.

[6] Zhang J, Chan-Park M B, Miao J and Sun T 2005 Reduction of diffraction effect for fabrication of very high aspect ratio microchannels in SU-8 over large area by soft cushion technology Microsyst. Technol. **11** 519-525.

[7] Anhoj T A, Jorgensen A M, Zauner D A and Hubner J 2006 The effect of soft bake temperature on the polymerization of SU-8 photoresist J. Micromech. Microeng. **16** 1819-1824.

[8] Ho C H, Chin K P, Yang C R, Wu H M and Chen S L 2002 Ultrathick SU-8 mold formation and removal, and its application to the fabrication of LIGA-like micromotors with embedded roots Sensor Actuat. A-Phys. **102** 130-138.

[9] Reynolds M, Elias A, Elliot D G, Backhouse C and Sameoto D 2012 Variation of thermal and mechanical properties of KMPR due to processing parameters J. Micromech. Microengg. **22** 125023.

[10] Brunet M, O' Donnell T, O' Brien, J McCloskey P, O' Mathúna S C 2002 Thick photoresist development for the fabrication of high aspect ratio magnetic coils J. Micromech. Microengg. **12** 444-9.

[11] Lee H, Lee K, Ahn B, Xu J, Xu L and Oh KW 2011 A new fabrication process for uniform SU-8 thick photoresist structures by simultaneously removing edge bead and air bubbles J. Micromech. Microengg. **21** 1250006.

[12] Du L, Liu Y and Li C 2011 Mechanism analysis of ultrasonic treatment on SU-8 in UV-LIGA technology Micro Nano Lett., **11** 900-3.

[13] Jeyaseelan A V and Rohan J F 2009 Fabrication of three-dimensional substrates for Li microbatteries on Si Appl. Surf. Sci. **256** s61-4.

[14] Bourrier D, Ghannam A, Dilhan M, Granier H 2014 Potential of BPN as a new negative photoresist for very thick layer high aspect ratio 2014 Microsyst. Technol. **20** 2089-96.

[15] Walker R, Sirotkin E, Schmueser I, Terry J G, Smith S, Stevenson J T M, Walton A J 2013 Characterisation and integration of parylene as an insulating structural layer for high aspect ratio electroplated copper coils *Proc. IEEE Inter. Conf. Microelectronics Test Structures (ICMTS)* pp 7-12.

[16] Galle P, Kim S H, Shag U and Allen MG 2010 Micromachined capacitors based in automated multilayer electroplating *Proc. IEEE Micromech. Syst. (MEMS)* pp. 332-335.

[17] Anthony R, Wang N, Kulkarni S and O' Mathúna C 2014 Advances in planar coil processing for improved micro-inductor performance IEEE T. Magn. **50** 1-4.

[18] Anthony R, Kulkarni S, Wang N and O' Mathúna C 2014 Advanced processing for high efficiency inductors for 2.5 D/ 3D power supply in package *Proc. IEEE 3D Syst. Integration Conf. (3DIC)* pp. 1-4.

[19] Greiner F, Quednau S, Dassinger F, Sarwar R, Schlaak H F, Guttmann M and Meyer P 2013 Fabrication techniques for multiscale 3D-MEMS with vertical metal micro- and nanowire integration J. Micromech. Microengg. **23** 025018.

[20] Wang N, O' Donnell T, Roy S, McCloskey P and O' Mathúna C 2007 Micro-inductors integrated on silicon for power supply on chip J. Magn. Magn. Mater. **316** e233-37.